IN SEARCH OF SUSY *

W. DE BOER

Institut für Experimentelle Kernphysik, University of Karlsruhe
D-7500 Karlsruhe, Germany

(Received April 21, 1997)

Electroweak precision tests of the SM and MSSM as well as Searches for Supersymmetric Particles and Higgs bosons at LEP II and their significance within the MSSM are discussed.

PACS numbers: 12.60. Jv, 13.85. Rm

1. Introduction

Although at present the Standard Model (SM) shows good agreement with all available data, many questions can only be answered by assuming new physics beyond the SM. An excellent candidate for new physics is the supersymmetric extension of the SM (MSSM), which was found to describe the electroweak data equally well. In addition the MSSM allows

- Unification of the gauge coupling constants;
- Unification of the Yukawa couplings;
- Natural occurrence of the Higgs mechanism at a low scale;
- Cancellation of the quadratic divergences in the radiative corrections of the SM
- Relic abundance of dark matter.

After the discovery that unification within the SM is excluded by the precise measurements of the coupling constants at LEP I [1–3], a flood of papers on these subjects have emerged. Some recent contributions of the groups involved are given in Refs [4–12] It is surprising that one can find a region of parameter space within the *minimal* SUSY model, where all the independent constraints mentioned above can be fulfilled simultaneously.

* Presented at the Cracow Epiphany Conference on W Boson, Cracow, Poland, January 4–6, 1997.

The paper has been organized as follows: first the electroweak precision tests of the SM and MSSM are discussed, followed by the corresponding restrictions on the MSSM parameter space, both from the searches and the unification conditions.

2. Electroweak precision tests of the SM and MSSM

In this section an equivalent analysis of all electroweak data, both in the SM and its supersymmetric extension, is described using all actual electroweak data from Tevatron, LEP and SLC [13], the measurement of $\mathrm{BR}(b \to s\gamma)/\mathrm{BR}(b \to ce\bar{\nu})$ from CLEO [14] and limits on the masses of supersymmetric particles. The observed $b \to s\gamma$ decay rate is 30% below the SM prediction, while the decay $Z_0 \to b\bar{b}$ is about 1.8σ above the SM prediction. In the MSSM light stops and light charginos increase R_b [15–23] and decrease the $b \to s\gamma$ rate, so both observations can be brought into agreement with the MSSM for the same region of parameter space. However, as will be shown, the resulting χ^2 value for the MSSM fits is only marginally lower. In addition, the splitting in the stop sector has to be unnaturally high, so it remains to be seen if these effects are real or due to a fluctuation. Further details of the procedure and extensive references are given elsewhere [24].

2.1. Standard model fits

The SM cross sections and asymmetries are completely determined by $M_Z, m_t, m_H, G_F, \alpha, \alpha_s$. From the combined CDF and D0 data m_t has been determined to be 175 ± 6 GeV [25], so the parameters with the largest uncertainties are m_H and α_s. The error on the finestructure constant α is limited by the uncertainty in the hadronic cross section in e^+e^- annihilation at low energies, which is used to determine the vacuum polarization contributions to α. The error was taken into account by considering α to be a free parameter in the fit and constraining it to the value $1/\alpha = 128.89 \pm 0.09$ [26]. If this error is not taken into account, the error on the Higgs mass is underestimated by 30%. Using the input values discussed in the introduction yields:

$$\begin{aligned} \alpha_s &= 0.120 \pm 0.003\,, \\ m_t &= 172.0^{+5.8}_{-5.7}\ \mathrm{GeV}\,, \\ m_H &= 141^{+140}_{-77}\ \mathrm{GeV}\,. \end{aligned}$$

Minor deviations from the EWWG fit results [13] are due to the incorporation of the $b \to s\gamma$ data from CLEO [14], which are important for

the MSSM fits described below. From the SM fit parameters one can derive the value of the electroweak mixing parameter in the $\overline{\rm MS}$ scheme: $\sin^2\theta_{\overline{\rm MS}} = 0.2316 \pm 0.0004$, which is within errors equal to $\sin^2\Theta_{\rm eff}^{\rm lept}$. The main contributions to the χ^2/d.o.f = 18.5/15 originate from $\sin^2\Theta_{\rm eff}^{\rm lept}$ from SLD ($\Delta\chi^2 = 4.9$), R_b ($\Delta\chi^2 = 3.1$) and $A_{\rm FB}^b$ ($\Delta\chi^2 = 3.5$), but the overall SM agreement is good: the χ^2/d.o.f.=18.5/15 corresponds to a probability of 24%.

The low value of $\sin^2\Theta_{\rm eff}^{\rm lept}$ from SLD as compared to the LEP value yields a Higgs mass below the lower limit on the SM Higgs mass from direct searches, as demonstrated in Fig. 1. The LEP data alone without SLD yield $m_H \approx 240$ GeV, while $\sin^2\Theta_{\rm eff}^{\rm lept}$ from SLD corresponds to $m_H \approx 15$ GeV, as indicated by the squares in Fig. 1. The latter value is excluded by the 95% C.L. lower limit of 63.9 GeV from the LEP experiments [27,28]. The different values of $\sin^2\Theta_{\rm eff}^{\rm lept}$ from LEP and SLD translate into different predictions for M_W, as shown in Fig. 2. The present M_W measurements, including the preliminary value from the LEP II measurements [29] lie in between these predictions.

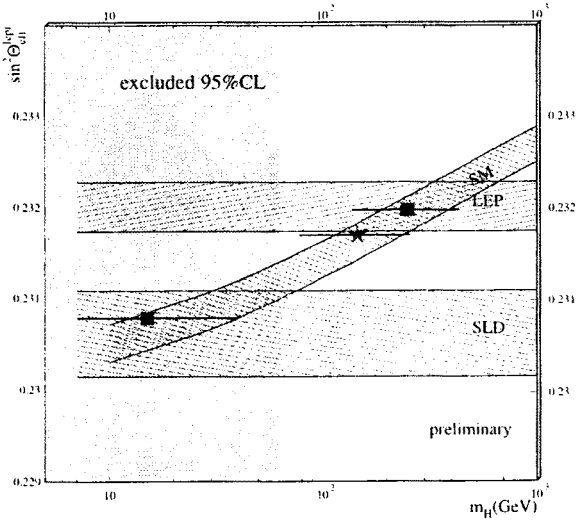

Fig. 1. Dependence of the SM $\sin^2\Theta_{\rm eff}^{\rm lept}$ on the Higgs mass. The top mass $m_t = 175 \pm 6$ GeV was varied within its error, as shown by the dashed band labelled SM. The SLD and the LEP measurements of $\sin^2\Theta_{\rm eff}^{\rm lept}$ are also shown as horizontal bands. The SLD value yields a Higgs mass below the recent limits by direct Higgs searches at LEP (shaded area).

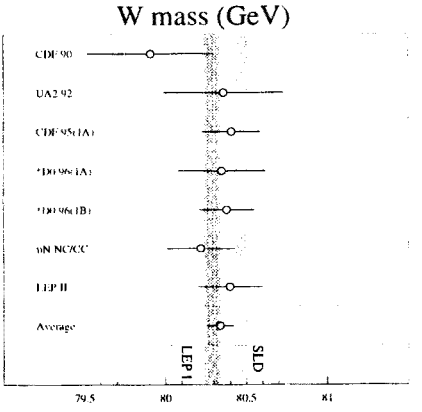

Fig. 2. A compilation of the W-masses. The vertical lines indicate the predictions from the LEP I and SLD electroweak data determining $\sin^2\Theta_{\rm eff}^{\rm lept}$ and the data points represent the various direct measurements of M_W.

2.2. MSSM fits and comparison with the SM

As mentioned in the introduction, the MSSM can increase the value of R_b, which experimentally is slightly above the SM value. The major additional contributions originate from vertex contributions with light charginos and light right handed stops in the low $\tan\beta$ scenario and light higgses for large $\tan\beta$ values. Since the large $\tan\beta$ scenario does not improve R_b significantly [24], it will not be discussed here anymore. The R_b dependence on chargino and stop masses is shown in Fig. 3. The experimental value $R_b = 0.2178 \pm 0.0011$ is clearly above the SM value of 0.2158 and can be obtained for charginos around 85 GeV and the lightest stop mass around 50 GeV (best fit results, [24]), although the second stop mass has to be heavy, *i.e.* well above m_t.

As will be discussed in the next section, such a large splitting in the stop sector is difficult to obtain in the MSSM, if one requires unification of the left and right-handed stop squarks at the GUT scale. Final analysis of available LEP data will teach of the present preliminary value of R_b will indeed stay above the SM value.

The fit results are compared with the Standard Model fits in Fig. 4. The Standard Model χ^2/d.o.f. = 18.5/15 corresponds to a probability of 24%, the MSSM χ^2/d.o.f. = 16.1/12 to a probability of 19%. In counting the d.o.f. the insensitive (and fixed) parameters were ignored [24].

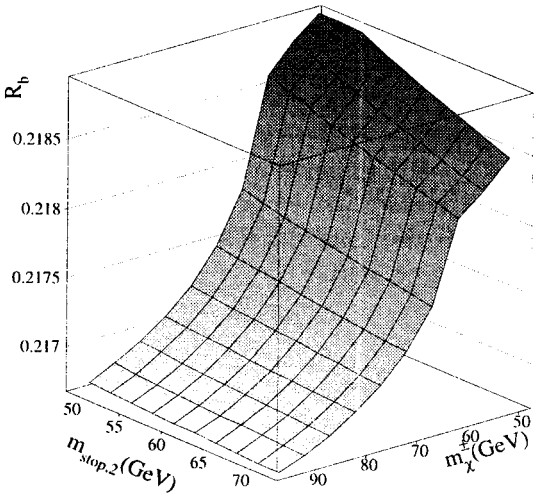

Fig. 3. R_b as function of the stop and chargino masses for $\tan\beta = 1.6$. The experimental value $R_b = 0.2178 \pm 0.0011$ is clearly above the SM value of 0.2158 and can be obtained for light charginos and stops.

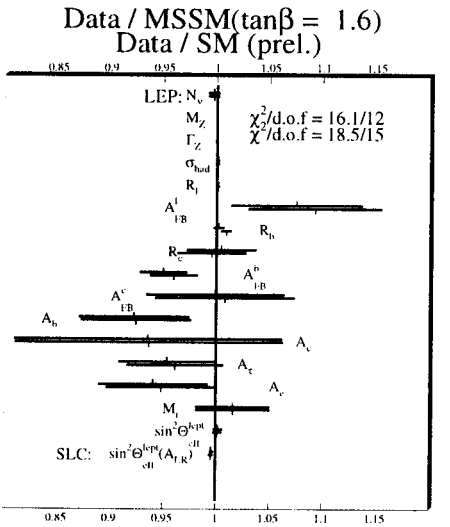

Fig. 4. Fit results normalized to the SM- and MSSM ($\tan\beta = 1.6$) values. The difference in $\chi^2/d.o.f$ between the SM and MSSM originates mainly from $\sin^2\Theta^{\rm lept}_{\rm eff}$, $A^b_{\rm FB}$ and R_b.

It is interesting to note that the predicted value of m_W tends to be higher in the MSSM than in the SM, especially for light stops, as shown in Fig. 5.

Another interesting point are the $\alpha_s(M_Z)$ values. An increase in R_b implies in increase in the total width of the Z^0 boson, which can be compensated by a decrease in the QCD corrections, *i.e.* α_s. However, since R_b is only marginally above the SM value, the fitted value of $\alpha_s(M_Z)$ between SM and MSSM is within the error bars. Note that the α_s crisis has disappeared after the LEP value from the total cross section came down and the value from both lattice calculations and deep inelastic scattering went up [30].

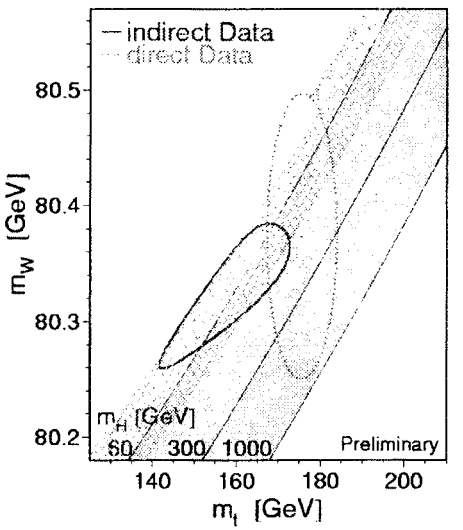

Fig. 5. m_W and m_t from direct (Tevatron and LEP II) and indirect measurements in comparison with the SM (shaded area) and MSSM (crossed area) predictions. The uncertainty from the SM prediction originates from the unknown Higgs mass, while for the MSSM it is mainly the uncertainty from the stop mass, since the Higgs mass is quite well predicted in the MSSM. The highest m_W mass is obtained for the lightest stop mass.

3. The Minimal SuperSymmetric Model (MSSM)

Supersymmetry presupposes a symmetry between fermions and bosons, which can only be realized in nature by assuming for every particle of the SM with spin j a supersymmetric partner (sparticles) with spin $j - 1/2$. These spartners must have the same mass and couplings as the particles, if supersymmetry is an exact symmetry in nature. However, since the spar-

ticles have not been observed sofar, supersymmetry must be broken. The MSSM can be obtained from the SM by replacing the known fields with the superfields, which include the spin 0 sfermions and the spin 1/2 gauginos.

In addition supersymmetry requires two complex SU(2) doublets for the Higgs sector instead of only one in the SM. The reasons are twofold: *(i)* in the SM one can give mass to the down-type quarks and leptons by using the complex conjugate of the Higgs doublet. Since the Higgses in the MSSM are part of the bosonic fields, one cannot just take the complex conjugate of just a part of the superfield structure, so one needs separate Higgs doublets for up- and down-type fermions. *(ii)* the superpartners of the Higgses are fermions, which contribute the triangle anomalies, unless the total hypercharge equals zero. This requires the introduction of two SU(2) Higgs doublets with opposite hypercharge.

Since the top quark is much heavier than the bottom quark, the Yukawa corrections for the two mass terms of the two Higgs doublets are very different, thus breaking the symmetry between them. These radiative corrections automatically lead to the Higgs mechanism of spontaneous electroweak symmetry breaking at a scale far below the unification scale, as discussed in many reviews [4].

Another difference between the interactions in the SM and MSSM arises from the triple vertices: in the SM a spin 1/2 fermion cannot couple to two other fermions, since this would violate conservation of angular momentum (or more general Lorentz invariance). For spin 0 particles such triple vertices are allowed, so fermions can couple to a sfermion and a fermion! Such vertices with three fermions violate lepton and/or baryon number. They can be avoided in the MSSM by introducing an additional multiplicative quantum number, called R-parity, defined as:

$$R = (-1)^{3(B-L)+2S}. \tag{3.1}$$

This quantity is +1 for SM particles and -1 for the supersymmetric partners, because of the change in the spin S. R-parity conservation forbids the coupling of a fermion to a sfermion and fermion, since the final state would have $R = -1\ \{.\}\ \{+1\} = -1$, thus eliminating the dangerous baryon — and lepton number violating vertices. It is usually assumed that R-parity is conserved exactly, since the experimental limits on the R-parity violating couplings are very severe. R-parity conservation implies that:

- sparticles can only be produced in pairs
- the lightest supersymmetric particle is stable, since its decay into normal matter would violate R-parity.
- the interactions of particles and sparticles can be different. For example, the photon couples to electron-positron pairs, but the photino does

not couple to selectron-spositron pairs, since in the latter case the R-parity would change from -1 to +1. In other words, each triple vertex must have 2 sparticles attached to it, thus forbidding the triple vertices in which a fermion couples to a sfermion and another fermions.

Obviously SUSY cannot be an exact symmetry of nature; else the supersymmetric partners would have the same mass as the normal particles. In the absence of a fundamental understanding of the origin of supersymmetry breaking one considers all breaking terms, which do not introduce quadratic divergences. This cancellation between fermions and bosons in the loop corrections is one of the great advantages of the MSSM, since it allows one to calculate radiative corrections up to the unification scale without divergences.

The breaking terms consist of the gaugino mass terms, the scalar mass terms, the trilinear (A-term) interactions amongst the scalars and the analogous bilinear (B-term) interactions [31].

If one assumes that SUSY is broken due to the *universal* gravitational interactions one needs only a *few* independent SUSY breaking parameters at the unification scale: a common mass $m_{1/2}$ for the gauginos, a common mass m_0 for the scalars, a common trilinear interaction A_0 and a bilinear coupling B_0.

In addition to these soft breaking terms one needs to specify the ratio $\tan\beta$ of the two Higgs VEVs and a supersymmetric Higgsino mixing parameter μ. The minimization conditions of the Higgs potential requiring a non-trivial minimum for electroweak symmetry breaking [32] yields a relation between the bilinear coupling B_0 and $\tan\beta$ and determines the value of μ^2, so finally the SUSY mass spectrum in this supergravity inspired scenario is determined by the following parameters:

$$m_0,\ m_{1/2},\ \tan\beta,\ A_0,\ \mathrm{sign}(\mu) \tag{3.2}$$

As will be shown in the next section, $\tan\beta$ has only two solutions from the known top mass, while $sign(\mu)$ and A_0 do not influence the mass spectrum strongly (except for the mixing in the stop sector, which can change the lightest Higgs mass by 10-15 GeV), so the main variables for the prediction of the SUSY mass spectrum are m_0 and $m_{1/2}$. The various MSSM masses and couplings have to be evolved via the renormalization group equations (RGE) from their common value at the unification scale to the electroweak scale. This involves solving typically 26 coupled differential equations with common values as boundary conditions at M_{GUT} $(t = \ln(M/M_{\mathrm{GUT}})^2 = 0)$:

$$\text{scalars}: \quad \tilde{m}_Q^2 = \tilde{m}_U^2 = \tilde{m}_D^2 = \tilde{m}_L^2 = \tilde{m}_E^2 = m_0^2; \tag{3.3}$$

$$\text{gauginos}: \quad M_i = m_{1/2}, \quad i = 1,2,3; \tag{3.4}$$

$$\text{couplings}: \quad \tilde{\alpha}_i(0) = \tilde{\alpha}_{GUT}, \quad i = 1,2,3. \tag{3.5}$$

Here M_1, M_2, and M_3 are the gauginos masses of the U(1), SU(2) and SU(3) groups. One has, however, to take into account the mixing between various states.

3.1. Gaugino-higgsino mass terms: charginos and neutralinos

Gauginos and Higgsinos both have spin $j = 1/2$, so the mass eigenstates can be different from the interaction eigenstates because of the non-diagonal mass terms. The partners of the two neutral gauge bosons and two neutral Higgs bosons are the four neutralinos $\tilde{\chi}_i^0$ $(i = 1, 4)$ after mixing; correspondingly, the charginos $\tilde{\chi}_i^{\pm}$ $(i = 1, 2)$ are mixtures of the wino and charged higgsino. The neutralino mixing is described by the following mass matrix:

$$M^{(0)} = \begin{pmatrix} M_1 & 0 & -M_Z \cos\beta \sin_W & M_Z \sin\beta \sin_W \\ 0 & M_2 & M_Z \cos\beta \cos_W & -M_Z \sin\beta \cos_W \\ -M_Z \cos\beta \sin_W & M_Z \cos\beta \cos_W & 0 & -\mu \\ M_Z \sin\beta \sin_W & -M_Z \sin\beta \cos_W & -\mu & 0 \end{pmatrix}. \tag{3.6}$$

The physical neutralino masses $M_{\tilde{\chi}_i^0}$ are obtained as eigenvalues of this matrix after diagonalization. For charginos one has similarly:

$$M^{(c)} = \begin{pmatrix} M_2 & \sqrt{2} M_W \sin\beta \\ \sqrt{2} M_W \cos\beta & \mu \end{pmatrix}. \tag{3.7}$$

The M_1 and M_2 terms are the gaugino masses at low energies. They are linked to their common values at the GUT scale ($m_{1/2}$) by the RGE group equations. Numerically one finds at the weak scale:

$$M_3(\tilde{g}) \approx 2.7 m_{1/2}, \tag{3.8}$$

$$M_2(M_Z) \approx 0.8 m_{1/2}, \tag{3.9}$$

$$M_1(M_Z) \approx 0.4 m_{1/2}, \tag{3.10}$$

$$\mu(M_Z) \approx 0.63 \mu(0). \tag{3.11}$$

Since the gluinos obtain corrections from the strong coupling constant α_3, they grow heavier than the gauginos of the $SU(2) \otimes U(1)$ group.

In the case favoured by the fit discussed below one finds $\mu \gg M_2 > M_W$, in which case the charginos eigenstates are approximately M_2 and μ and the four neutralino mass eigenstates are $|M_1|, |M_2|, |\mu|$, and $|\mu|$, respectively. In other words, the neutralinos and charginos do not mix strongly, so the lightest chargino is wino-like, while the LSP is bino-like, which has consequences for dark matter searches.

3.2. Squark and slepton masses

The non-negligible Yukawa couplings cause a mixing between the electroweak eigenstates and the mass eigenstates of the third generation particles. The mixing matrix for the stopsector is:

$$\begin{pmatrix} \tilde{m}_{tL}^2 & m_t(A_t - \mu \cot \beta) \\ m_t(A_t - \mu \cot \beta) & \tilde{m}_{tR}^2 \end{pmatrix}. \tag{3.12}$$

The mass eigenstates are the eigenvalues of this matrix. Similar matrices exist for sbottom and stau, except that in the off-diagonal elements m_t is replaced by $m_{b(\tau)}$ and $\cot \beta$ is replaced by $\tan \beta$, so the mixing effects are smaller, unless $\tan \beta$ is large. For the first and second generation the mixing can be neglected, since the off-diagonal terms are proportional to the quark masses of the first and second generation.

The squark and slepton masses are assumed to all have the same value at the GUT scale. However, in contrast to the sleptons, the squarks get radiative corrections from virtual gluons which make them heavier than the sleptons at low energies.

3.3. CMSSM and R_b

An increase in R_b requires one (mainly right handed) stop to be light and the other one to be heavy (see previous section). If both would be light, then all other squarks are likely to be light, which would upset the good agreement between the SM and the electroweak data. A large mass splitting in the stop sector needs a very artificial fine tuning of the few free parameters in the Constrained MSSM, which connects unified masses and couplings at the GUT scale to their values at the electroweak scale via RGE, as will be discussed in the next section. This is obvious from the mixing matrix in the squark sector (see 3.12): if one of the diagonal elements is much larger than m_t, the off-diagonal terms of the order m_t will not cause a mixing and the difference between the left- and right-handed stops has to come from the evolution of the diagonal terms, which depend on the Yukawa couplings for top and bottom (Y_t, Y_b) and the trilinear couplings $A_{t(b)}$. For low $\tan \beta$ Y_b is negligible, while A_t and Y_t are not free parameters, since they go to fixed point solutions [33], *i.e.* become independent of their values at the GUT scale. Therefore there is little freedom to adjust these parameters within the CMSSM in order to get a large splitting between the left- and right-handed stops.

In addition, problems arise with electroweak symmetry breaking, since this requires the Higgs mixing parameter μ to be much heavier than the

gaugino masses [33], while R_b requires low values of μ for a significant enhancement (since the chargino has to be preferably Higgsino-like). In conclusion, within the CMSSM an enhancement of R_b above the SM is practically excluded; only if all squark and gaugino masses are taken as free parameters without considering the RGE and common values at the GUT scale, then one can obtain an improvement in R_b.

4. Low energy constraints in the CMSSM

Within the Constrained Minimal Supersymmetric Model (CMSSM) it is possible to predict the low energy gauge couplings and masses of the 3 generation particles from the few supergravity inspired parameters at the GUT scale. The main ones are m_0 and $m_{1/2}$ as discussed in Section 3, Eq. 3.2. Moreover, the CMSSM predicts electroweak symmetry breaking due to large radiative corrections from the Yukawa couplings, thus relating the Z^0 boson mass to the top quark mass via the renormalization group equations (RGE). In addition, the cosmological constraints on the lifetime of the universe are considered in the fits. The new precise measurements of the strong coupling constant and the top mass as well as higher order calculations of the $b \to s\gamma$ rate exclude perfect fits in the CMSSM, although the discrepancies from the best fit parameters are below the 2σ level.

TABLE I

Summary of input data and fit parameters for the global fit from Ref. [35]. All parameters were fitted simultaneously in order to take care of the correlations, but the GUT scale $M_{\rm GUT}$ and corresponding coupling constant $\alpha_{\rm GUT}$ are mainly determined from gauge coupling unification, $\tan\beta$ and the Yukawa couplings $Y^0_{(t,b,\tau)}$ at the GUT scale from the masses of the 3th generation, and μ from electroweak symmetry breaking (EWSB). For the low $\tan\beta$ scenario the trilinear coupling A_0 is not very relevant, but for large $\tan\beta$ it is determined by $b \to s\gamma$ and $b\tau$-unification. The scalar- and gaugino masses $(m_0, m_{1/2})$ enter in all observables.

input data	$\Rightarrow$	Fit parameters
$\alpha_1, \alpha_2, \alpha_3$	min.	$M_{\rm GUT}$, $\alpha_{\rm GUT}$
m_t, m_b, m_τ	χ^2	Y^0_t, $Y^0_b = Y^0_\tau$
M_Z		m_0, $m_{1/2}$, μ, $\tan\beta$
$b \to s\gamma$		A_0
$\tau_{\rm universe}$		

In this analysis the coupling constants were taken from the fits described in the first section. The new higher order calculations for the important $b \to s\gamma$ rate indicate that next to leading log (QCD) corrections increase

the SM value by about 10% [34]. This can be simulated in the lowest level calculation by choosing a renormalization scale $\mu = 0.65 m_b$, which will be done in the following. Here we repeat an update of a previous analysis [35] with the new input values mentioned above. The input data and fitted parameters have been summarized in Table I.

4.1. Constraints from gauge coupling unification

The most restrictive constraints are the coupling constant unification and the requirement that the unification scale has to be above 10^{15} GeV from the proton lifetime limits, assuming decay via s-channel exchange of heavy gauge bosons. They exclude the SM [2] as well as many other models [36,37].

4.2. Constraints from the top mass

In the MSSM the top mass is given by:

$$m_t^2 = 4\pi Y_t v^2 \frac{\tan^2 \beta}{1 + \tan^2 \beta} . \tag{4.1}$$

The top Yukawa coupling Y_t is given by the RGE, which shows a *fixed point* behaviour, *i.e.* its low energy value is independent of its value at the GUT scale [4], but only determined by the known *gauge* couplings. Since the VEV of the Higgs field $v = 174$ GeV is known from the Z^0 mass, all parameters except $\tan \beta$ are known, so the MSSM predicts the top (pole) mass to be:

$$m_t^2 \approx (205 \text{ GeV})^2 \sin^2 \beta . \tag{4.2}$$

The maximum possible topmass is around 205 GeV and a top mass of 175 GeV corresponds to $\tan \beta \approx 1.5$, as shown in the top part of Fig. 6. For large values of $\tan \beta$ the bottom and τ Yukawa couplings become large too (see middle part of Fig. 6) and the top Yukawa coupling cannot be predicted from the gauge couplings alone. However, if one assumes $b - \tau$ unification ($Y_b = Y_\tau$ at the GUT scale), one finds a second large $\tan \beta$ solution, as shown in the top part of Fig. 6 too, so for $m_t = 175 \pm 6$ GeV only two regions of $\tan \beta$ give an acceptable χ^2, as shown in the bottom part of Fig. 6.

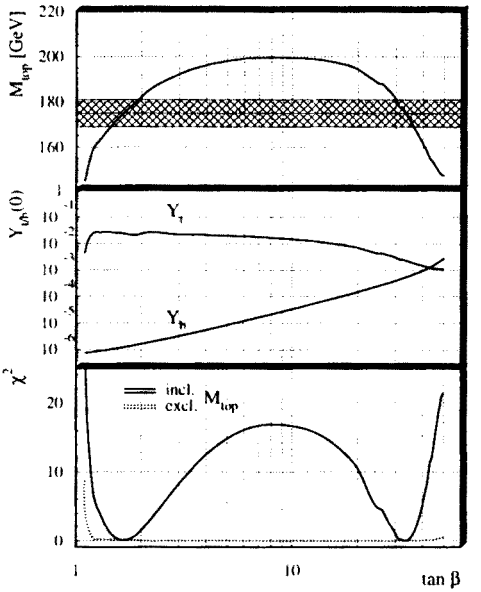

Fig. 6. The top quark mass as function of $\tan\beta$ (top). The middle part shows the corresponding values of the Yukawa couplings at the GUT scale and the lower part the χ^2 values. For $\tan\beta < 20$ the Yukawa coupling of the b-quark Y_b is small compared to Y_t, in which case the top quark mass is given by the infrared fixed point solution of Y_t. For large values of $\tan\beta$ Y_t is reduced by the negative corrections from Y_b and Y_τ, which were assumed to have common values at the GUT scale ($b - \tau$ unification). If the top constraint ($m_t = 175 \pm 6$, horizontal band) is not applied, all values of $\tan\beta$ are allowed (thin dotted lines at the bottom), but if the top mass is constrained to the experimental value, only the regions around $\tan\beta \approx 1.7$ and $\tan\beta \approx 35$ are allowed.

4.3. Electroweak Symmetry Breaking (EWSB)

Radiative corrections can trigger spontaneous symmetry breaking in the electroweak sector. In this case the Higgs potential does not have its minimum for all fields equal zero, but the minimum is obtained for non-zero vacuum expectation values of the fields. Minimization of the Higgs potential yields:

$$\frac{M_Z{}^2}{2} = \frac{m_1^2 + \Sigma_1 - (m_2^2 + \Sigma_2)\tan^2\beta}{\tan^2\beta - 1}, \tag{4.3}$$

where $m_{1,2}$ are the mass terms in the Higgs potential and Σ_1 and Σ_2 their radiative corrections. Note that the radiative corrections are needed, since unification at the GUT scale with $m_1 = m_2$ would lead to $M_Z < 0$. In order

to obtain $M_Z > 0$ one needs to have $m_2^2 + \Sigma_2 < m_1^2 + \Sigma_1$ which happens at low energy since Σ_2 (Σ_1) contains large negative corrections proportional to Y_t (Y_b) and $Y_t \gg Y_b$. Electroweak symmetry breaking for the large $\tan\beta$ scenario is not so easy, since Eq. 4.3 can be rewritten as:

$$\tan^2\beta = \frac{m_1^2 + \Sigma_1 + \frac{1}{2}M_Z^2}{m_2^2 + \Sigma_2 + \frac{1}{2}M_Z^2}. \tag{4.4}$$

For large $\tan\beta$ $Y_t \approx Y_b$, so $\Sigma_1 \approx \Sigma_2$ (see Fig. 6). Eq. 4.4 then requires the starting values of m_1 and m_2 to be different in order to obtain a large value of $\tan\beta$, which could happen if the symmetry group above the GUT scale has a larger rank than the SM, like e.g. SO(10) [38]. In this case the quartic interaction (D-) terms in the Higgs potential can generate quadratic mass terms, if the Higgs fields develop non-zero VEVs after spontaneous symmetry breaking.

Alternatively, one has to assume the simplest GUT group SU(5), which has the same rank as the SM, so no additional groups are needed to break SU(5) and consequently no D-terms are generated. In this case EWSB can only be generated, if Y_b is sufficiently below Y_t, in which case the different running of m_1 and m_2 is sufficient to generate EWSB. The resulting SUSY mass spectrum is not very sensitive to the two alternatives for obtaining $m_1^2 + \Sigma_1 > m_2^2 + \Sigma_2$: either through a splitting between m_1 and m_2 already at the GUT scale via D-terms or by generating a difference via the radiative corrections.

4.4. Discussion of the remaining constraints

In Fig. 7 the total χ^2 distribution is shown as a function of m_0 and $m_{1/2}$ for the two values of $\tan\beta$ determined above. One observes minima at $m_0, m_{1/2}$ around (200,270) and (800,90), as indicated by the stars. These curves were still produced with the data from last year. With the new coupling constants one finds slightly different minima, as given in Table II. In this case the minimum χ^2 is not as good, since the fit wants $\alpha_s \approx 0.125$, i.e. about 1.6σ above the measured LEP value and the calculated $b \to s\gamma$ rate is above the experimental value too, if one takes as renormalization scale $\mu \approx 0.65 m_b$. At this scale the next higher order corrections, as calculated by [34], are minimal. The contours in Fig. 7 show the regions excluded by different constraints used in the analysis:

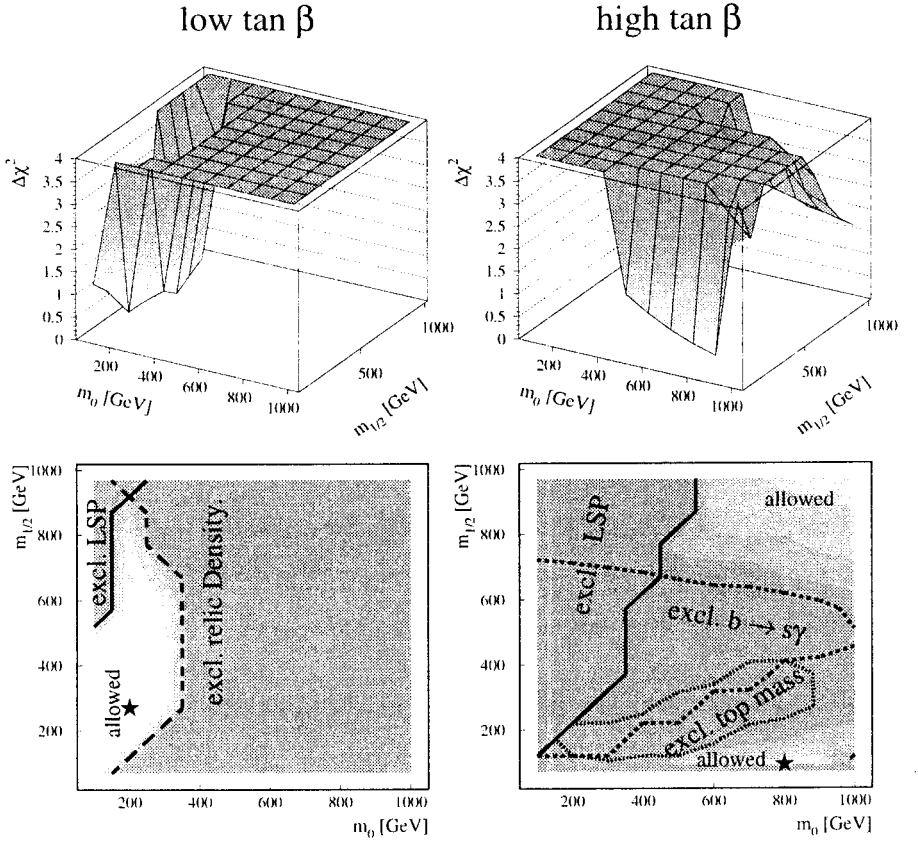

Fig. 7. Contours of the χ^2-distribution for the low and high $\tan\beta$ solutions in the m_0 versus $m_{1/2}$ plane. The different shades indicate steps of $\Delta\chi^2 = 1$, so basically only the light shaded region is allowed. The stars indicate the optimum solution. Contours enclose domains excluded by the particular constraints used in the analysis.

TABLE II

Values of the fitted SUSY parameters (upper part) and corresponding susy masses (lower part) for low and high $\tan\beta$ solutions using the new input data discussed in the text.

Fitted SUSY parameters and masses in GeV		
Symbol	**low** $\tan\beta$	**high** $\tan\beta$
m_0, $m_{1/2}$	230, 225	850, 115
$\mu(M_Z)$, $\tan\beta$	-880, 1.7	-190, 30
$Y_t(m_t)$, $A_t(M_Z)$	0.008, -370	0.006, 86
$\tilde{\chi}_1^0$, $\tilde{\chi}_2^0$	96, 194	47, 92
$\tilde{\chi}_3^0$, $\tilde{\chi}_4^0$	509, 519	414, 417
$\tilde{\chi}_1^\pm$, $\tilde{\chi}_2^\pm$	194, 518	92, 422
$\tilde{g}$, $\tilde{q}$, $\tilde{l}$	558, 545, 563	300, 885, 854
h, H	74, 673	109, 624
A, $H^\pm$	680, 684	624, 630

4.5. LSP constraint

The requirement that the LSP is neutral excludes the regions with small m_0 and relatively large $m_{1/2}$, since in this case one of the scalar staus becomes the LSP after mixing via the off-diagonal elements in the mass matrix. The LSP constraint is especially effective at the high $\tan\beta$ region, since the off-diagonal element in the stau mass matrix is proportional to $A_t m_0 - \mu \tan\beta$.

4.6. $b \to s\gamma$ rate

At low $\tan\beta$ the $b \to s\gamma$ rate is close to its SM value for most of the plane. The charginos and/or the charged Higgses are only light enough at small values of m_0 and $m_{1/2}$ to contribute significantly. The trilinear couplings were found to play a negligible role for low $\tan\beta$. However, for large $\tan\beta$ the trilinear coupling needs to be left free, since it is difficult to fit simultaneously $b \to s\gamma$, m_b and m_τ. The reason is that the corrections to m_b are large for large values of $\tan\beta$ due to the large contributions from $\tilde{g} - \tilde{q}$ and $\tilde{\chi}^\pm - \tilde{t}$ loops proportional to $\mu\tan\beta$. They become of the order of 10-

20%. In order to obtain $m_b(M_Z)$ as low as 2.84 GeV, these corrections have to be negative, thus requiring μ to be negative. The $b \to s\gamma$ rate is too large in most of the parameter region for large $\tan\beta$, because of the dominant chargino contribution, which is proportional to $A_t\mu$. For positive (negative) values of $A_t\mu$ this leads to a larger (smaller) branching ratio $BR(b \to s\gamma)$ than for the Standard Model with two Higgs doublets. In order to reduce this rate one needs $A_t(M_Z) > 0$ for $\mu < 0$. Since for large $\tan\beta$ A_t does not show a fixed point behaviour, this is possible.

4.7. Relic density

The long lifetime of the universe requires a mass density below the critical density, else the overclosed universe would have collapsed long ago. This requires that the contribution from the LSP to the relic density has to be below the critical density, which can be achieved if the annihilation rate is high enough. Annihilation into electron-positron pairs proceeds either through t-channel selectron exchange or through s-channel Z^0 exchange with a strength given by the Higgsino component of the lightest neutralino. For the low $\tan\beta$ scenario the value of μ from EWSB is large [35]. In this case there is little mixing between the higgsino- and gaugino-type neutralinos as is apparent from the neutralino mass matrix: for $|\mu| \gg M_1 \approx 0.4m_{1/2}$ the mass of the LSP is simply $0.4m_{1/2}$ and the "bino" purity is 99% [35]. For the high $\tan\beta$ scenario μ is much smaller and the Higgsino admixture becomes larger. This leads to an enhancement of $\tilde{\chi}^0 - \tilde{\chi}^0$ annihilation via the s-channel Z boson exchange, thus reducing the relic density. As a result, in the large $\tan\beta$ case the constraint $\Omega h_0^2 < 1$ is almost always satisfied unlike in the case of low $\tan\beta$.

5. Discovery potential at LEP II

All LEP experiments have been searching for the sparticles and Higgs bosons predicted by the MSSM. Table II shows that charginos, neutralinos and the lightest Higgs belong to the lightest particles in the MSSM, so we will concentrate on these searches and show only a few typical results for each experiment keeping in mind that the other experiments have usually similar results on the same channel.

Charginos are expected to be easy to discover, since they will be pair produced with a large cross section of several *pb* and lead to events with characteristic decays similar to $W^{\pm}$ pairs plus missing energy. The typical limits are close to the beam limit, as shown in Fig. 8 by recent results from DELPHI [39]. Since the chargino mass depends on the SUSY parameters μ, M_2 and $\tan\beta$ these limits can be shown as contours in the $\mu - M_2$ plane for

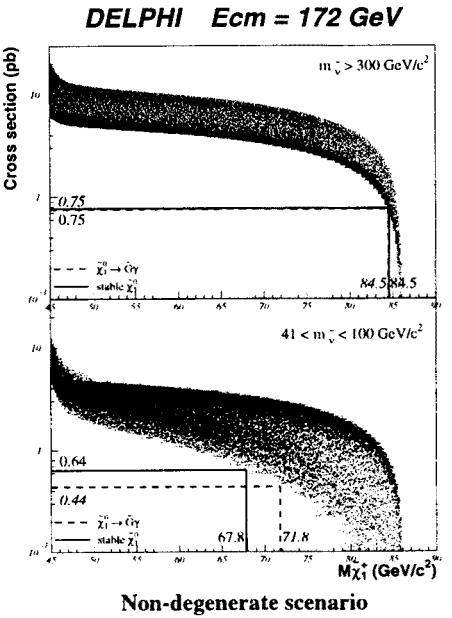

Fig. 8. Chargino limits from DELPHI for 4 different cases: for heavy sneutrinos with stable and unstable neutralinos the chargino mass is above 84.5 GeV at 95% C.L. (upper part); As indicated, the unstable neutralino is assumed to decay into a photon and gravitino. For light sneutrinos the negative interference between s- and t-channel reduces the cross section, thus leading to worse limits as shown in the bottom part. It is assumed that the lightest chargino is non-degenerate with the LSP. In case the lightest chargino is Higgsino-like, implying $\mu < M_2$ (see Eq. 3.7), the chargino can be degenerate with the LSP, but the t-channel sneutrino is suppressed in this case. If the degeneracy is less than 5 GeV, limits rather close to the kinematic limit are obtained. From [39].

a given value of $\tan\beta$, as shown in Fig. 9 for LEP data at 161 and 172 GeV centre of mass energies from OPAL [40]. If one assumes the GUT relation $M_2 \approx 2M_1$ (Eq. 3.11) the neutralino limits are related to the chargino limits. Combining it with direct neutralino searches, both at LEP I and LEP II, L3 finds a lower limit on the neutralino mass of 24.6 GeV [41] as shown in Fig. 10. The Higgs mass is a function of the pseudoscalar Higgs mass m_A, $\tan\beta$ and the topmass via the radiative corrections. Higgs bosons can be produced through Higgs-strahlung $e^+e^- \to hZ$ and associated production $e^+e^- \to hA$. The first one is proportional to $\sin^2(\beta-\alpha)$, while the second one to $\cos^2(\beta-\alpha)$, so the total cross section is independent of the mixing angles $\beta-\alpha$. If one searches for both processes one can find a Higgs limit independent of $\tan\beta$, as shown for the ALEPH data in Fig. 11 (from Ref. [42]).

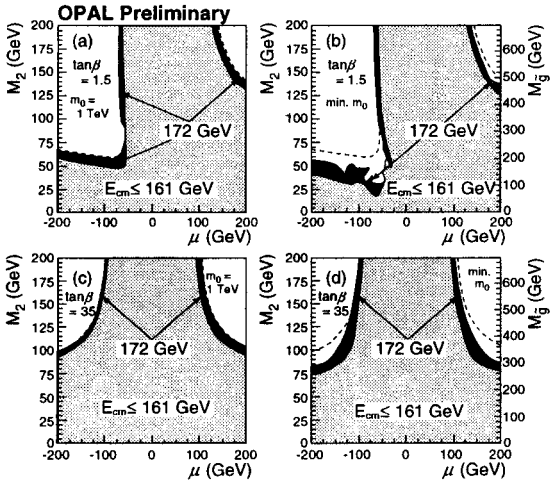

Fig. 9. M_2 versus μ from OPAL for LEP data from $\sqrt{s} = 161$ and 172 GeV. Note that for chargino/neutralino searches the reach in parameter space increases only linear with energy in contrast to the Higgs searches. From [40].

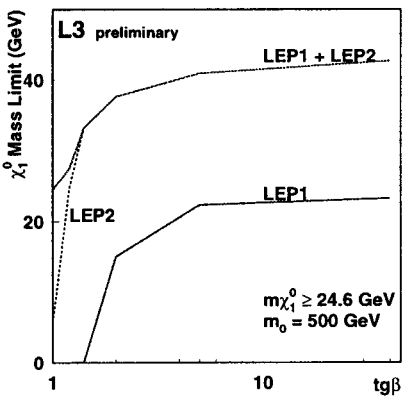

Fig. 10. The mass of the lightest stable neutralino, assumed to be the LSP, is related to the lightest chargino mass via the RGE equations, which connect common gaugino masses at the GUT scale to the electroweak scale. Combining the search limits of chargino and neutralino pair production leads to a lower mass limit of 24.6 GeV for the invisible LSP for all values of $\tan\beta$, provided the lightest sneutrino is heavy. For light sneutrinos the negative t- and s-channel interference reduce the chargino cross section, thus reducing the LSP limit. From [41].

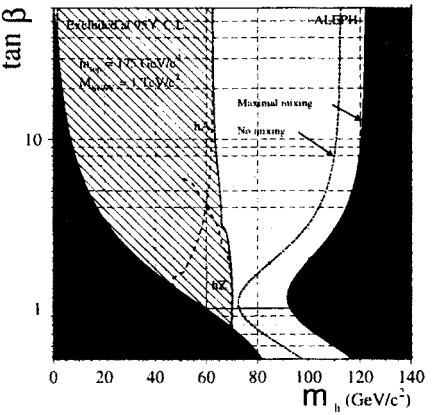

Fig. 11. $\tan\beta$ versus the Higgs mass from ALEPH [42]. The dashed area is excluded by the search for the hZ and hA final states, which require both m_h and m_A to be above 62.5 GeV at 95% C.L. The dark regions are excluded in case of large mixing in the stop sector, the solid line in case of no mixing. In the constrained MSSM the mixing is usually small, so for small $\tan\beta$ the combined data from all LEP experiments will exclude the low $\tan\beta$ scenario. The region for $2 < \tan\beta < 40$ is excluded from the solution of the RGE for the top Yukawa coupling, as shown in Fig. 6.

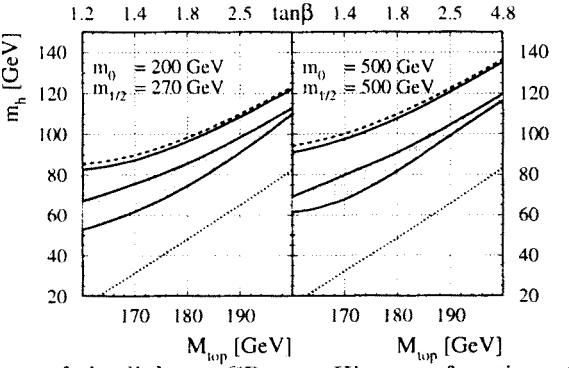

Fig. 12. The mass of the lightest CP-even Higgs as function of the top mass at Born level (dotted lines), including complete one-loop contributions of all particles (dashed lines). Two-loop contributions reduce the one-loop corrections significantly as shown by the dashed area (the upper boundary corresponds to $\mu > 0$, the lower one to $\mu < 0$). The solid line just below the dashed line is the one-loop prediction from the third generation only, which apparently gives the main contribution. The upper scale indicates the value of $\tan\beta$, as calculated from the top mass (Eq. 4.2).

The Higgs mass depends on the top mass as shown in Fig. 12. Here the most significant second order corrections to the Higgs mass have been incorporated [43], which reduces the Higgs mass by about 15 GeV [44]. In this case the Higgsmass is below 90 GeV, provided the top mass is below 180 GeV (see Fig. 12), which implies that the foreseen LEP energy of 192 GeV is sufficient to cover the whole parameter space.

5.1. Summary

In summary, in the Constrained Minimal Supersymmetric Model (CMSSM) the allowed region of the GUT scale parameters and the corresponding SUSY mass spectra for the low and high $\tan\beta$ scenario have been determined from a combined fit to the low energy data on couplings, quark and lepton masses of the third generation, the electroweak scale M_Z, $b \to s\gamma$, and the lifetime of the universe. The new precise determinations of the strong coupling constant $\alpha_s = 0.120 \pm 0.003$ are slightly below the preferred CMSSM fit value of about 0.125. In addition, the observed $b \to s\gamma$ value of $(2.32 \pm 0.6)10^{-4}$ is below the predicted value, at least for the SM $(3.2 \cdot 10^{-4})$ and the low $\tan\beta$ scenario of the MSSM.

The lightest particles preferred by these fits are charginos and higgses. The charginos are preferably light in case of the high $\tan\beta$ scenario, while the lightest higgs will be within reach of LEP II in case of the low $\tan\beta$ scenario (see Fig. 6). So the light $\tan\beta$ scenario of the CMSSM can be confirmed or excluded at LEP II (provided the top mass is indeed below 180 GeV), while the complete parameter space for the high $\tan\beta$ scenario will become only accessible at future accelerators.

It should be noted that recent speculation about evidence for SUSY from the $ee\gamma\gamma$ event observed by the CDF collaboration [45], the too high value of R_b [13,24] and the ALEPH 4-jet events [46] has not been confirmed sofar:

- if the single CDF $ee\gamma\gamma + E_{\text{miss}}$ event would originate from selectron pair production with the two gammas coming from neutralino decay into either the LSP or gravitino, one would expect anomalous inclusive $p\bar{p} \to \gamma\gamma + E_{\text{miss}} + X$ production, which has not been observed [47].
- The R_b anomaly is reduced to "a-less-than-2σ-effect" [13].
- The anomalous ALEPH 4-jet events have not been confirmed by the other three LEP Collaborations [48].

I want to thank my colleagues from the LEP groups for helpful discussions and/or making available data prior to publication, especially Glen Cowan, Ralf Ehret, Dmitri Kazakov, Michael Kobel, Sachio Komamyia, Marco Pieri, Silvie Rosier, Michael Schmitt, and Ulrich Schwickerath.

REFERENCES

[1] J. Ellis, S. Kelley, D. V. Nanopoulos, *Phys. Lett.* **B260**, 131 (1991).

[2] U. Amaldi, W. de Boer, H. Fürstenau, *Phys. Lett.* **B260**, 447 (1991).

[3] P. Langacker, M. Luo, *Phys. Rev.* **D44**, 817 (1991).

[4] For review and original references see: N.P.Nilles, *Phys. Rep.* **110**, 1 (1984); H.E.Haber, G.L.Kane, *Phys. Rep.* **117**, 75 (1985); R.Barbieri, *Riv. Nuovo Cim.* **11**, 1 (1988); W.de Boer, *Prog. Part. Nucl. Phys.* **33**, 201 (1994).

[5] G.G. Ross, R.G. Roberts, *Nucl. Phys.* **B377**, 571 (1992).

[6] M. Carena, S. Pokorski, C.E.M. Wagner, *Nucl. Phys.* **B406**, 59 (1993); M. Olechowski, S. Pokorski, *Nucl. Phys.* **B404**, 590 (1993); and private communication.

[7] F. Anselmo, L. Cifarelli, A. Peterman, A. Zichichi, *Nuovo Cimento* **105**, 1179 (1992) and references therein.

[8] S. Kelley, J.L. Lopez, D.V. Nanopoulos, H. Pois, K. Yuan, *Phys. Rev.* **D47**, 2468 (1993).

[9] W. de Boer, R. Ehret, D. Kazakov, *Z. Phys.* **C67**, 647 (1995).

[10] L. E. Ibáñez, G. G. Ross, CERN-TH-6412-92, (1992), appeared in *Perspectives on Higgs Physics*, G. Kane (Ed.), p. 229 and references therein.

[11] R. Arnowitt, P. Nath, *Phys. Rev. Lett.* **69**, 725 (1992); *Phys. Lett.* **B287**, 89 (1992); For a review, see P. Langacker, Univ. of Penn. Preprint, UPR-0539-T.

[12] G. L. Kane, C. Kolda, L. Roszkowski, J. D. Wells, *Phys. Rev.* **D49**, 6173 (1994).

[13] The LEP Coll., Cern Preprint CERN-PPE/96-183.

[14] CLEO-Collaboration, R. Ammar *et al.*, *Phys. Rev. Lett.* **74**, 2885 (1995).

[15] Proceedings of the Workshop Physics at LEP2 , Editors G. Altarelli, T. Sjöstrand, F. Zwirner, Vol.1, CERN 96-01.

[16] M. Boulware, D. Finnell, *Phys. Rev.* **D44**, 2054 (1991).

[17] P.H. Chankowski, S. Pokorski, *Nucl. Phys.* **B475**, 3 (1996).

[18] J. Ellis, J.L. Lopez, D.V. Nanopoulos, *Phys. Lett.* **B372**, 95 (1996).

[19] D. Garcia, J. Solà, *Phys. Lett.* **B354**, 335 (1995).

[20] G.L. Kane, R.G. Stuart, J.D. Wells, *Phys. Lett.* **B354**, 350 (1995).

[21] J.D. Wells, C. Kolda, G.L. Kane, *Phys. Lett.* **B338**, 219 (1993).

[22] D. Garcia, R. Jimenez, J. Solà, *Phys. Lett.* **B347**, 309 (1995); *Phys. Lett.* **B347**, 321 (1995).

[23] D. Garcia, J. Solà, *Phys. Lett.* **B357**,349 (1995).

[24] W. de Boer, A. Dabelstein, W. Hollik, W. Mösle, U. Schwickerath, Updated Global Fits of the SM and MSSM to Electroweak Precision Data, hep-ph/9609209 and references therein.

[25] F. Abe *et al.*, CDF Collaboration, *Phys. Rev. Lett.* **74**, 2626 (1995); S. Abachi *et al.*, DØ Collaboration, *Phys. Rev. Lett.* **74**, 2632 (1995), An updated top mass ($m_t = 175 \pm 6$ GeV/c^2) from the combined CDF and D0 data was given by P. Tipton, Invited talk at 28th Int. Conf. on High Energy Physics, Warsaw, July 1996.

[26] S. Eidelman, F. Jegerlehner, *Z. Phys.* **C67**, 585 (1995); H. Burkhardt, B. Pietrzyk, *Phys. Lett.* **B356**, 398 (1995).

[27] R.M. Barnett *et al.*, *Phys. Rev.* **D54**, 1 (1996).

[28] D. Buskulic *et al.*, ALEPH Coll. *Phys. Lett.* **B313**, 312 (1993).

[29] The Electroweak Working Group for the LEP Coll., M_W determinations presented at Moriond, Note LEPWWG 97-01, April 1997.

[30] M. Schmelling, Plenary talk at 28th Int. Conf. on High Energy Physics, Warsaw, July 1996.

[31] L. Girardello, M.T. Grisaru, *Nucl. Phys.* **B194**, 419 (1984).

[32] K. Inoue, A. Kakuto, H. Komatsu, S. Takeshita, *Prog. Theor. Phys.* **68**, 927 (1982); ERR. *Prog. Theor. Phys.* **70**, 330 (1983); L.E. Ibáñez, C. Lopéz, *Phys. Lett.* **126B**, 54 (1983); *Nucl. Phys.* **B233**, 511 (1984); L. Alvarez-Gaumé, J. Polchinsky, M. Wise, *Nucl. Phys.* **221**, 495 (1983); J. Ellis, J.S. Hagelin, D.V. Nanopoulos, K. Tamvakis, *Phys. Lett.* **125B**, 275 (1983); G.Gamberini, G. Ridolfi, F. Zwirner, *Nucl. Phys.* **B331**, 331 (1990).

[33] W. de Boer *et al.*, Combined Fit of Low Energy Constraints to Minimal Supersymmetry and Discovery Potential at LEP II, hep-ph/9603350; W. de Boer *et al.*, *Z. Phys.* **C67**, 647 (1995).

[34] C. Greub, T. Hurth, SLAC-PUB-7267, ITP-SB-96-46, hep-ph/9608449; M. Misiak, talk given at 28th Int. Conf. on High Energy Physics, Warsaw, July, 1996.

[35] W. de Boer *et al.*, *Z. Phys.* **C71**, 415 (1996).

[36] U. Amaldi, W. de Boer, P.H. Frampton, H. Fürstenau, J.T. Liu, *Phys. Lett.* **B281**, 374 (1992).

[37] H. Murayama, T. Yanagida, Preprint Tohoku University, TU-370 (1991); T.G. Rizzo, *Phys. Rev.* **D45**, 3903 (1992); T. Moroi, H. Murayama, T. Yanagida, Preprint Tohoku University, TU-438 (1993).

[38] H. Murayama, M. Olechowski, S. Pokorski, *Phys. Lett.* **B371**, 57 (1996) and ref. therein.

[39] F. Richard for the DELPHI Coll. Presented at the CERN seminar on Feb. 25th, 1997.

[40] S. Komamiya for the OPAL Coll. Presented at the CERN seminar on Feb. 25th, 1997.

[41] M. Pieri for the L3 Coll. Presented at the CERN seminar on Feb. 25th, 1997.

[42] G. Cowan for the ALEPH Coll. Presented at the CERN seminar on Feb. 25th, 1997.

[43] M. Carena *et al.*, hep-ph/9602250; P. Chankowski, S. Pokorski, J. Rosiek, *Phys. Lett.* **B281**, 100 (1992); M. Carena, J.R. Espinosa, M. Quiros, C.E.M. Wagner, CERN Preprint CERN-TH/95-45; M. Carena, M. Quiros, C.E.M. Wagner, CERN Preprint CERN-TH/95-157; R. Hempfling, A. Hoang, *Phys. Lett.* **B331**, 99 (1994).

[44] A.V. Gladyshev *et al.*, hep-ph/9603346 and references therein.

[45] S. Dimopoulos *et al.*, *Phys. Rev.* **D54**, 3283 (1996); S. Ambrosiano *et al.*, *Phys. Rev.* **D54**, 5395 (1996); **D55**, 1372 (1997); J.L. Lopez, D.V. Nanopoulos, *Phys. Rev.* **D55**, 4450 (1997); *Mod. Phys. Lett.* **A10**, 2473 (1996).

[46] ALEPH Coll., D. Buskulic *et al.*,*Z. Phys.* **C71**, 179 (1996); P.H. Chankowski, D. Choudhury, S. Pokorski, *Phys. Lett.* **B389**, 677 (1996); D. Kumar, R.M. Godbole, hep-ph/9605460.

[47] B. Carithers for the CDF Coll., Invited talk at the DPG-Tagung, March 20, 1997, Munich.

[48] D. Schlatter, Conclusions from the LEP WG on ALEPH 4-jet events, presented at the CERN Seminar on Feb. 25th, 1997.